Electronic and Magnetic Reconstructions in La_{0.7}Sr_{0.3}MnO_{3}/SrTiO_{3} Heterostructures: A Case of Enhanced Interlayer Coupling Controlled by the Interface

F. Y. Bruno, J. Garcia-Barriocanal, M. Varela, N. M. Nemes, P. Thakur, J. C. Cezar, N. B. Brookes, A. Rivera-Calzada, M. Garcia-Hernandez, C. Leon, S. Okamoto, S. J. Pennycook, and J. Santamaria

Electronic and magnetic reconstructions in $La_{0.7}Sr_{0.3}MnO_3$/$SrTiO_3$ heterostructures: a case of enhanced interlayer coupling controlled by the interface.

F.Y. Bruno[1], J. Garcia-Barriocanal[1-2], M. Varela[3], N. M. Nemes[1], P. Thakur[4], J. C. Cezar[4], N. B. Brookes[4], A. Rivera-Calzada[1], M. Garcia-Hernandez[5], C. Leon[1], S. Okamoto[3], S. J. Pennycook[3], J. Santamaria[1].

[1] *GFMC. Dpto. Física Aplicada III, Universidad Complutense de Madrid, 28040 Madrid, Spain*

[2] *SpLine Spanish CRG Beamline at the ESRF, 6 rue Jules Horowitz, B.P. 220, F-38043 Grenoble Cedex, France*

[3] *Materials Science and Technology Division, Oak Ridge National Laboratory, Oak Ridge, Tennessee 37831-6071, USA*

[4] *European Synchrotron Radiation Facility (ESRF), 6 rue Jules Horowitz, B.P. 220, F-38043 Grenoble Cedex, France*

[5] *Instituto de Ciencia de Materiales de Madrid. Consejo Superior de Investigaciones Científicas. 28049 Cantoblanco Spain*

ABSTRACT:

We report on the magnetic coupling of LSMO layers through STO spacers in LSMO/STO epitaxial heterostructures. Combined aberration corrected microscopy and EELS spectroscopy evidence charge transfer to the empty conduction band of the

titanate. Ti d- electrons interact via superexchange with Mn giving rise to a Ti magnetic moment as demonstrated by x-ray magnetic circular dichroism. This induced magnetic moment in the STO controls the bulk magnetic and transport properties of the superlattices when the titanate layer thickness is below 1 nm.

Among correlated electron systems, $La_{0.7}Sr_{0.3}MnO_3$ (LSMO) has been extensively studied as a possible source of spin polarized electrons at room temperature [1]. The large values of tunnelling magnetoresistance (TMR) reported for $LSMO/SrTiO_3$ (STO) /LSMO tunnel junctions at low temperature drop way below the Curie temperature of the magnetic electrodes, suggesting that a depolarisation of the injected current may occur at the interface [2, 3]. This effect has been attributed to deteriorated magnetic properties of the manganite layer at the interface, a so called "dead layer", the origin of which is still not well understood [4, 5]. Modified electronic and orbital structures at the interface [6, 7] could be at the origin of the dead layer problem. In this paper we examine the possibility of manipulating the spin structure of the "dead layer" through the orbital reconstruction at the interface.

The origin of novel electronic states at the interface has been discussed in terms of the combined effect of epitaxial strain and the electronic and orbital reconstruction resulting from symmetry breaking [8-10]. Since in these correlated oxides spin ordering is largely determined by the orbital structure through Goodenough-Kanamori rules[11, 12], the modified bonding at the interface determines its magnetic structure. This is the case for the ferromagnetic state reported to occur at the interface between non-ferromagnetic $LaFeO_3$ and $LaCrO_3$ [13] and is also the origin of a ferromagnetic moment found in Cu at cuprate/manganite heterostructures [14, 15], in Fe at

BiFeO$_3$/LSMO interfaces [16] and very recently at the interface between the Mott insulator LaMnO$_3$ and the band insulator STO [17].

Here we show that manganite layers are magnetically coupled in LSMO/STO superlattices when the STO layer is thinner than 1 nm, which gives rise to very significant changes of magnetic and conducting properties. We have examined the electronic and magnetic structure of the LSMO/STO interface and found a magnetic moment induced at the Ti, resulting from the orbital reconstruction, which couples magnetically the LSMO layers. This finding constitutes direct evidence on how macroscopic properties of a heterostructure may be controlled by the interface orbital and spin reconstruction.

Using a high-pressure pure oxygen sputtering technique, we have grown two series of [LSMO$_M$/STO$_N$]$_8$ superlattices consisting of 8 bilayers of M LSMO unit cells (u.c.) and N STO u.c., on (100) STO substrates. In the first series of samples the LSMO thickness was fixed at M=6, thin enough to highlight the interface effects, with N$_{STO}$ = 0, 1, 2, 5, 6, 12, 18, 24. In the second series the STO thickness is fixed at N=2, with M$_{LSMO}$=4, 6, 14. X-ray reciprocal space maps show that the LSMO layers are uniformly strained (in plane) to match the lattice parameters of the STO (see SM Figure 1).

We first show the unusual magnetic and transport properties of the heterostructures. The temperature dependence of (van der Pauw) resistivity and magnetization are shown in Figure 1 for a thin film and three superlattices with STO thickness N = 2, 7 and 18 u.c. These measurements are normalized to the LSMO thickness which is the same for all samples. We find a strong, 2 orders of magnitude,

increase of the metallic state resistivity when the STO thickness is increased. The application of 14 T has a pronounced effect in reducing the low temperature resistance of samples with STO thicker than 7 u.c., showing that the degraded magnetic and transport properties of the samples with thick STO are related to a disordered spin structure in the LSMO. This may be the origin of the widely reported "dead layer". Electronic transport and magnetic properties at low temperature in manganites are linked by the double exchange mechanism where the hopping amplitude of electrons between neighboring Mn atoms is proportional to $cos(\theta_{ij}/2)$ where θ_{ij} is the angle between the localized t_{2g} spins. A fully magnetized sample in a 14 T field (well above the saturation magnetic field) has all the spins aligned and, thus, ought not to present low temperature magnetoresistance. However, if the spins on the Mn sites are misoriented, then the application of a magnetic field should align them with a concomitant decrease in resistivity. The magnetoresistance of the 48 u.c. LSMO thin film at 10K is only 2%, and in the case of the $[LSMO_6/STO_2]_8$ superlattice it reaches 10% (Fig. 1(a)). These low values of magnetoresistance are consistent with ordered (parallel) spin states which can also be deduced from the fact that the saturation magnetization (M_S) of these samples is 3.7 μ_B/at_{Mn} the full theoretical spin only moment (Fig. 1(c)). However, the superlattices with thick STO have much larger magnetoresistance at 10K, 70% for $[LSMO_6/STO_7]_8$ and $[LSMO_6/STO_{18}]_8$, evidencing a disordered spin state in these samples consistent with the values of M_S=2.5 μ_B/at_{Mn} observed. For samples with thick STO we obtain T_C=200K while in the case of the $[LSMO_6/STO_2]_8$ sample the T_C increases up to 280K accompanying the increased magnetization shown. For a thin film 6 u.c. thick the obtained values of saturation magnetization and Curie temperature are M_S^{TF}=1.5μ_B/at_{Mn} and T_C^{TF}=150K, similar to those of the heterostructures with STO thicker than 5 u.c. Thus multilayers with thick

STO behave like the sum of isolated LSMO layers whereas with thin STO the whole heterostructure determines the properties showing that there exists some substantial coupling between the layers. This is a striking result in view of the insulating and non magnetic nature of the STO and suggests that a significant interface reconstruction may be taking place. An enhancement of the magnetic moment has been also observed in LMO/STO superlattices when STO thickness is reduced [19]. However, since LMO (ferro) magnetism depends strongly on strain relaxation, an explanation in terms of the same sort of magnetic coupling discussed later is not straightforward.

To examine possible changes in doping due to interface charge transfer we have examined the interface chemistry by combined aberration corrected microscopy and electron energy loss spectroscopy. Figure 2(a) shows a high magnification Z contrast STEM image of a single $[LSMO_6/STO_N]_{10}$ superlattice where N varies between 2 u.c. and 8 u.c. along the stack and there are two bilayers for each STO thickness. Coherent heteroepitaxial growth of LSMO and STO is observed with sharp interfaces free of defects (see also supplementary figures SM1 and SM2). In simultaneous EELS experiments, the Ti-$L_{2,3}$, Mn-$L_{2,3}$, La-$M_{4,5}$ and Sr $L_{2,3}$, edges were recorded to produce the relative concentration profile of Fig. 2(b) and elemental maps from the first two STO layers are shown in Fig. 2 (c-f). The LSMO (STO) layer looks chemically wider in the La(Ti) image than in the Mn (Sr) map indicating that both interfaces are TiO_2 terminated[18], with an extra $La_{0.7}Sr_{0.3}O$ layer at the interface. In the thicker region, interface roughness develops and the termination appears to alternate between the top and bottom interfaces. EELS elemental maps yield insights into the oxidation state of the different species through the dependence of the shape of these absorption edges on band filling. Figure 2(b) (bottom) shows the oxidation state of the transition metal oxide

(TMO), obtained from the O K edge fine structure, through the energy separating the pre-peak and the main peak [19, 20]. This method implies some averaging of both LSMO and STO signals at the interfaces due to electron beam broadening, not taken into account by the error bars. Nevertheless, the general trend is clear; Fig. 2(b) shows how the Ti oxidation state evolves from $Ti^{3.7+}$ when the STO is 2 u.c. thick to stoichiometric Ti^{4+} when the STO is 8 u.c. thick. While it is quite clear that Ti atoms in the bulk of the layer are in a 4+ oxidation state when the bilayer index (and the STO layer thickness) increases, while the interfacial Ti in the thin STO layers exhibits a reduced oxidation state. The Mn oxidation state remains constant and around 3.2+, less than the 3.3+ nominal stoichiometry. The reduced Ti oxidation state in ultrathin STO layers is consistent with an electronic reconstruction at the manganite-titanate interface. The extra $La_{0.7}Sr_{0.3}O$ layer at the interface would provide a nominal extra 1/3 e^- per interfacial TiO_2 plane reducing the Ti oxidation state [19]. La-Sr intermixing could also cause the reduced oxidation state of Ti. However, this can be excluded for at least two reasons: in Fig 2(d) negligible La signal is detected in the STO layer, and furthermore, electron doping of STO caused by La enrichment implies a hole enrichment of the LSMO near the interface, which is not observed. The reduced Mn oxidation state (3.2+ vs the nominal 3.3+) possibly indicates a small density (2%) of O vacancy doping. Since the layers are uniformly strained, changes observed in magnetic and transport properties cannot be explained in terms of a change in strain state. We can also rule out that changes in the magnetotransport properties are due to a modified doping level of the manganite due to oxygen vacancies, because the Mn oxidation state is constant when the STO thickness is modified along the superlattice.

Motivated by the recent finding of induced magnetism at the interface between the Mott insulator $LaMnO_3$ and the band insulator $SrTiO_3$(STO) [17] we have explored the magnetic properties of the LSMO/STO interface. Figure 3(a) shows XMCD spectra at the Mn and Ti L edge of $[LSMO_6/STO_2]_8$ at 6 K in a 1 T magnetic field, conducted at the ID08 Beamline of the European Synchrotron Radiation Facility (ESRF). The Mn XMCD signal of 27% is consistent with previous studies on LSMO/STO interfaces [21]. Remarkably, a clear dichroic signal is also observed at the Ti edge demonstrating the ferromagnetic character of STO, although bulk STO is a diamagnetic band insulator. The origin of the Ti magnetism is seen in the temperature dependence in Fig. 3(b): The Ti magnetic moment follows the Mn moment, both in temperature and magnitude (inset) demonstrating that the origin of the Ti moment is interaction with the Mn moment. A rough estimate of the magnitude of the magnetic moment of Ti M_s= -0.04μ_B/at$_{Ti}$ was obtained by applying sum rules [22]. The negative value of the Ti moment means that its direction is opposite to the magnetic field, and hence that the Mn-Ti coupling is antiferromagnetic. This calculated value can be considered a lower bound because sum rules applied to early transition metal oxides are known to seriously underestimate the moment due to the small spin orbit splitting of the $2p_{1/2}$ and $2p_{3/2}$ core levels[23]. The present case is fundamentally different from previous reports of interfacial magnetism involving LSMO like the case of Cu [14] or Fe [16] where the interfacial magnetism is a consequence of a reordering of pre-existing (antiferromagnetic) moments, because here no magnetic moment is expected on Ti atoms for an empty Ti^{4+} d-band. Since the t_{2g} orbitals in STO are located slightly above the Fermi level of the manganite, orbital hybridisation may drive an electronic reconstruction at this interface [24]. In particular, we propose a scenario where hybridized "down" $d_{xz,yz}$ bonding orbitals reside lower in energy than hybridized "up"

bonding $d_{3z^2-r^2}$ orbital. This hybridized-orbital picture is a natural consequence of the lattice mismatch between STO and LSMO and the reduced electron density in LSMO compared with undoped $LaMnO_3$. The former increases the energy level of the bonding $d_{3z^2-r^2}$ orbital, and the latter suppresses the occupation of the bonding $d_{3z^2-r^2}$ orbital. These effects cooperatively destabilize the ferromagnetic coupling via either the double-exchange or superexchange interaction mediated by the $d_{3z^2-r^2}$ orbital[17]. Because of the charge transfer occurring at this interface and electron doping by the $La_{0.7}Sr_{0.3}O$ layer, Ti is in a mixed 3+/4+ oxidation state at the interface, resulting in the antiferromagnetic coupling with respect to Mn.

We now discuss the enhanced magnetization and transport of the samples with ultrathin spacers ($[LSMO_6/STO_2]_8$) in terms of a magnetic coupling mechanism mediated by the Ti induced magnetism. Ti atoms at the interface are antiferromagnetically aligned to Mn moments in the LSMO probably as a consequence of the hybridization process of Ti $d_{xz,\,yz}$ orbitals. These electrons residing in $d_{xz,\,yz}$ orbitals at the interface provide a mechanism for the magnetic coupling of the manganite layers if the STO layer is thin enough. The effect of coupling is to order the interface spins and so to increase the saturation magnetization and Curie temperature and to reduce the low temperature magnetoresistance. The physical mechanism of the coupling could be through direct exchange by free carriers of the STO spreading into 1-2 unit cells [25] or by a ferromagnetic superexchange mechanism between t_{2g} electrons that may be allowed by Goodenough-Kanamori rules in single occupied orbitally degenerate t_{2g} orbitals. Although we also detect a magnetic moment at interfacial Ti in samples with thicker STO layers, this magnetism is confined to the interface as in this

case there are no electrons in the d band of Ti in the bulk of the STO layers. This suppresses magnetic coupling for thick STO.

In summary we have found a magnetic coupling between LSMO layers through (nominally insulating and diamagnetic) STO spacers. This interaction originates at the electronic reconstruction occurring at the interface between LSMO and STO. Charge is transferred to the empty conduction band of the titanate and as a consequence the oxidation state of the Ti is reduced as shown by EELS measurements. An XMCD experiment evidences that the Mn-O-Ti superexchange interaction at the interface induces a magnetic moment in Ti. This provides the channel for the magnetic interaction between LSMO layers when the STO is thinner than 1 nm resulting in the magnetic coupling of the manganite layers and a suppression of the magnetic dead layer. The bulk magnetic and transport properties are then determined by this interfacial spin reconstruction.

FIGURE CAPTIONS

Fig. 1. (color online). (a) Temperature dependent resistivity of $[LSMO_6/STO_N]_8$ superlattices in 14 T (open symbols) and zero (solid symbols) field. (b) Temperature dependent magnetization upon warming in 100 Oe. N is indicated in the figures. (c) M(H) loops measured in a vibrating sample magnetometer (VSM). (d) sketch

illustrating magnetic coupling through interfacial Ti in the case of an ultrathin STO spacer.

Fig. 2. (color online). (a) High magnification Z-contrast image of a $[LMSO_6/STO_N]$ superlattice where the STO layer thickness is varied between 2 and 8 u.c., thickness is indicated in the figure. (b) Top: normalized integrated intensity of Ti-$L_{2,3}$(blue), Mn-$L_{2,3}$(red), La $M_{4,5}$(green) along the direction marked with a green arrow on (a). Bottom: Mn (red) and Ti (blue) oxidation states. The blue lines are guides to the eye. (c-f) Atomic elemental maps corresponding to the (c) Ti $L_{2,3}$, (d) Mn $L_{2,3}$, (e) La $M_{4,5}$, (f) Sr $L_{2,3}$ signals, after fitting the background to a power law and integrating 30 eV wide windows under the remaining edges, except for (f) where a 300 eV wide window was used due to the poor signal. Datasets in (a,b) obtained in a VG Microscopes HB501UX, while datasets in (c-f) were obtained in the Nion UltraSTEM, both operated at 100 kV and equipped with aberration correctors and Gatan Enfina spectrometers.

Fig. 3. (color online). XMCD measurements in an $[LMSO_6/STO_2]_8$ superlattice. (a) Ti $L_{2,3}$ edge (red) Mn $L_{2,3}$ edge (green). For comparison, the Ti signal is multiplied by 10. (b) Temperature dependent Ti (green open circles) and Mn (red full circles) intensities and magnetization (black line), all normalized at 4K. (inset) Maximum intensity of Ti (at 466 eV) vs. Mn (at 642 eV) XMCD signal for $[LMSO_N/STO_2]_8$, N=2, 4 and 14. The red line is a linear fit.

[1]   J. Park *et al.*, Nature (London) **392**, 794 (1998).
[2]   V. Garcia *et al.*, Phys. Rev. B **69**, 052403 (2004).
[3]   M. Bowen *et al.*, Appl. Phys. Lett. **82**, 233 (2003).
[4]   H. Yamada *et al.*, Science **305**, 646 (2004).
[5]   M. Izumi *et al.*, Phys. Rev. B **64**, 064429 (2001).
[6]   H. Yamada *et al.*, Appl. Phys. Lett. **89**, 052506 (2006).
[7]   A. Tebano *et al.*, Phys. Rev. Lett. **100**, 137401 (2008).
[8]   Y. Tokura, and N. Nagaosa, Science **288**, 462 (2000).
[9]   S. Okamoto, and A. Millis, Nature (London) **428**, 630 (2004).
[10]   J. Mannhart, and D. Schlom, Science **327**, 1607 (2010).
[11]   J. B. Goodenough, Phys. Rev. **100**, 564 (1955).
[12]   J. Kanamori, J. Phys. Chem. Solids **10**, 87 (1959).
[13]   K. Ueda, H. Tabata, and T. Kawai, Science **280**, 1064 (1998).
[14]   J. Chakhalian *et al.*, Nature Phys. **2**, 244 (2006).
[15]   J. Chakhalian *et al.*, Science **318**, 1114 (2007).

[16]   P. Yu *et al.*, Phys. Rev. Lett. **105**, 027201 (2010).

[17]   J. Garcia-Barriocanal *et al.*, Nat. Comm. **1**, 82 (2010).

[18]   J. Maurice *et al.*, Philos. Mag. **86**, 2127 (2006).

[19]   J. Garcia-Barriocanal *et al.*, Adv. Mater. **22**, 627 (2010).

[20]   M. Varela *et al.*, Phys. Rev. B **79**, 085117 (2009).

[21]   J. J. Kavich *et al.*, Phys. Rev. B **76**, 014410 (2007).

[22]   C. Chen *et al.*, Phys. Rev. Lett. **75**, 152 (1995).

[23] C. Piamonteze, P. Miedema, and F. M. F. de Groot, Phys. Rev. B **80**, 184410 (2009).

[24]   S. Okamoto, Phys. Rev. B **82**, 024427 (2010).

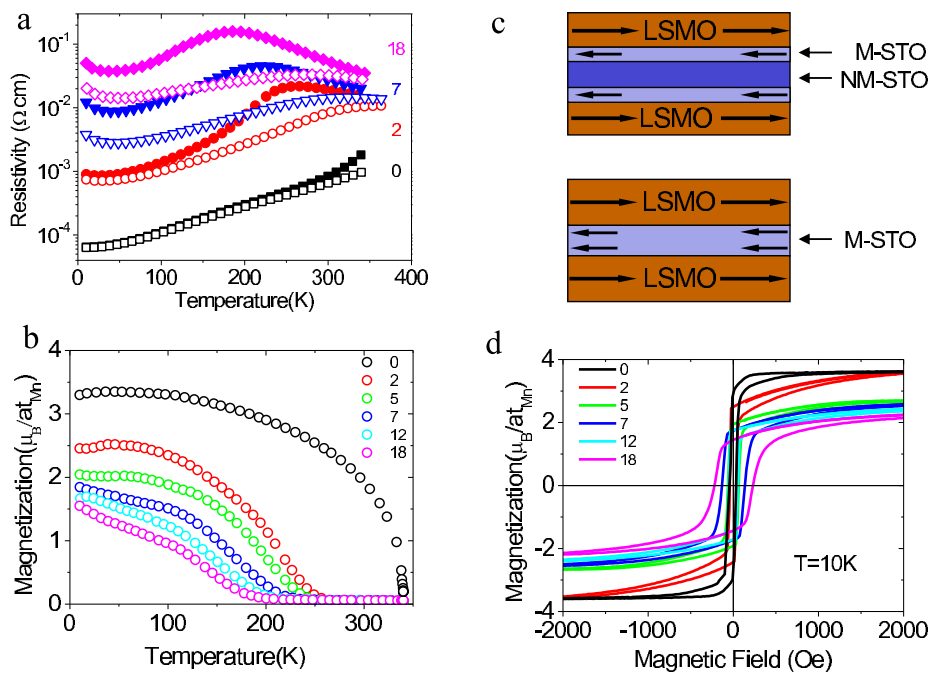[25]   G. Herranz *et al.*, Phys. Rev. Lett. **96**, 027207 (2006).
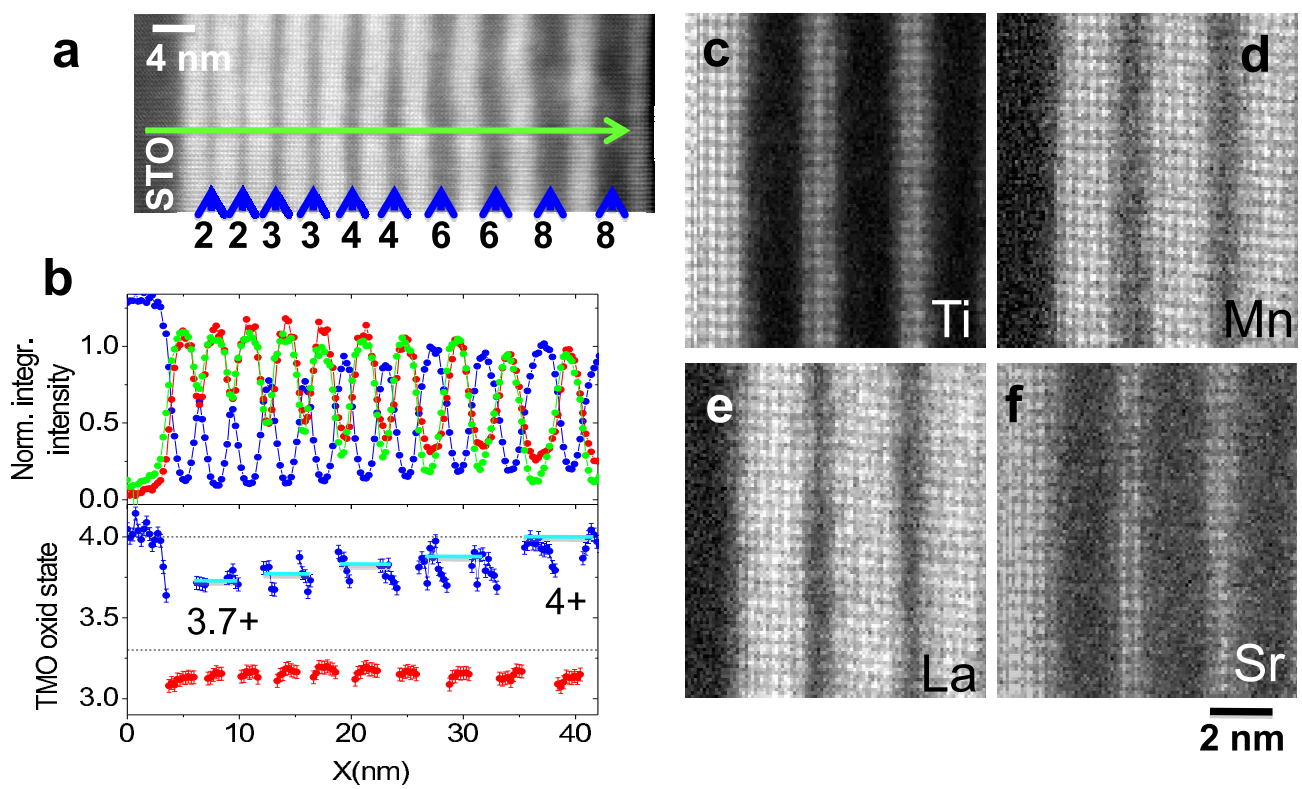
Fig. 1. F.Y. Bruno *et al.*

Figure 1   LZ12126   11MAR2011
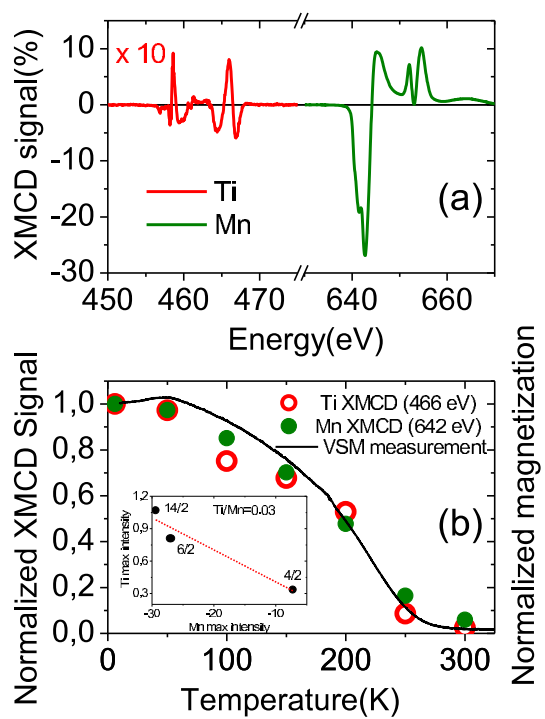
Fig. 2. F.Y. Bruno *et al.*

Figure 2   LZ12126   11MAR2011

Fig. 3. F.Y. Bruno *et al.*

Figure 3   LZ12126   11MAR2011